IEEE Robotics and Automation Letters (RAL) paper presented at the
2020 IEEE/RSJ International Conference on Intelligent Robots and Systems (IROS)
October 25-29, 2020, Las Vegas, NV, USA (Virtual)

Precision Assembly of Heavy Objects Suspended with Multiple Cables From a Crane

Rachel Hoffman[1], H. Harry Asada[2]

***Abstract*— A new approach to precision mating of heavy objects suspended from overhead cranes is presented. We have found through experiments that heavy shafts suspended with multiple cables at specific positions and orientations can be inserted into a chamfered hole despite a small clearance. This will allow an overhead crane, although limited in positioning accuracy, to execute precision assembly of a heavy shaft simply by holding it with multiple cables and lowering it onto the chamfered hole of a fixed object. Unlike the well-known Remote Center Compliance (RCC) hand, this method does not use a two-layer elastic structure but exploits the physical properties of cables. Specifically, cables go slack when a compressive load is applied. This unidirectional load bearing property is exploited to suspend a heavy shaft such that it is not over-constrained during insertion. Conditions for the cable attachment position and orientation for successful insertion are obtained. A proof-of-concept prototype is developed and experimental verification of the principle and analysis are presented.**

Assembly, Industrial Robots, Factory Automation

I. INTRODUCTION

Accurate positioning of heavy sub-assemblies and structures is a challenging task in heavy industry. Fine positioning and mating of crane-hung objects requires special experience, and is largely dependent on skilled labor. Workers standing near a crane-hung object carefully adjust the position and orientation of the object by directly pushing and pulling it while adjusting the height of the crane such that the object is aligned with a reference. The hung object must be lowered at the right position and orientation so that it can be seated in the structure correctly. This requires the coordination of the crane for lowering the object and the adjustment of the object location within a horizontal plane. To perform these operations quickly, many years of experience are required. Moreover, industries have been facing difficulties in recruiting young people for these highly-skilled positions because modern society deems them Dirty, Dangerous, Demeaning, and Difficult, termed 4D works [1].

Therefore, there is a specific need for automating the process by which heavy objects (greater than 25Kg) can be manipulated, specifically focusing on precision alignment and mating processes. Due to existing factory setups, it is strongly desired that existing overhead cranes be utilized to manipulate the heavy work-pieces. Although gigantic industrial robots capable of handling heavy objects weighing up to 1300kg are available [2], those robots themselves take up a significant amount of floor space despite low utility, and the work space must be fenced for safety.

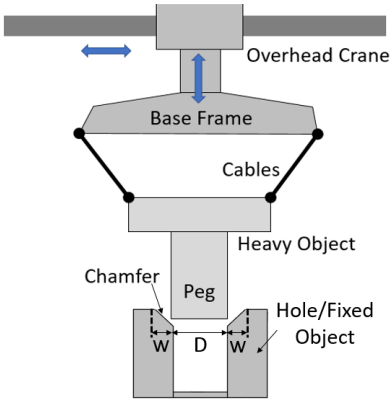

Fig. 1. Overhead crane manipulating a suspended heavy peg/shaft. The overhead crane can position the base frame within a few millimeters of accuracy, but is not accurate enough to insert the peg into the hole on its own.

This work aims to manipulate heavy objects by combining a cable driven parallel robotic system with current overhead crane technology. Cable driven parallel robotic systems are known for high load-to-weight ratio, large work spaces, and multi-axis control up to 6 degrees of freedom [3]. There are several prior works in which cable driven systems were developed to work in factories and manipulate heavy objects [4]–[7]. One successful example of a cable driven system integrated with a gantry crane is the NIST RoboCrane [4]. The RoboCrane is essentially an inverted Stewart platform parallel link manipulator with cables and winches serving as the links and actuators, respectively. The platform is kinematically constrained by maintaining tension in all six cables that terminate in pairs at the vertices of an upper support triangle. This arrangement allows for 6-DOF teleoperated force and position control to perform precision tasks, such as grinding, object manipulation and sawing [8]. While these prior works have addressed many important tasks, peg insertion precision assembly has never been reported. Other than standard pick and place operations, to the authors knowledge, there has not been any work investigating the requirements for performing assembly tasks, specifically peg insertion, using an underconstrained cable suspended platform.

Manuscript received: February 24, 2020; Revised June 3, 2020; Accepted July 5, 2020.

This paper was recommended for publication by Editor Dan Popa upon evaluation of the Associate Editor and Reviewers' comments. This work was supported by Sumitomo Heavy Industries.

[1]Rachel Hoffman is with Department of Mechanical Engineering at the Massachusetts Institute of Technology rachelmh@mit.edu

[2]H. Harry Asada is faculty in Department of Mechanical Engineering at the Massachusetts Institute of Technology asada@mit.edu

Digital Object Identifier (DOI): see top of this page.

In the prior works, due to the desire for accurate cartesian positioning, it is generally undesirable for any of the cables in these systems to go slack. The workspace analysis and control strategies for these systems explicitly avoid the situations where cables go slack. There appears to be an unexplored area of cable suspended system in which the use of slack is exploited to obtain additional system compliance, thus avoiding over-constraining the peg during insertion.

The peg-in-hole problem has been addressed extensively since the mid 70's. Several famous works [9]–[12] pioneered the Remote Center Compliance (RCC) hand, which provided a simple, elegant solution to the precision insertion problem. Holding a peg with a two-layered compliant structure, they have shown that the peg can be aligned towards the center of the hole while being guided across a chamfer surface and thereby inserted without causing jamming and wedging. The method has been applied to various assembly works for small-to-medium size work-pieces. One primary challenge of peg-in-hole insertion is the correct application and proportion of insertion forces. If the system actuating the peg position and orientation applies insertion forces in the incorrect proportions, the peg may jam or wedge itself in the hole [13].

The RCC end-effector with a compliant structure is difficult to apply to the assembly of large, heavy objects used in the heavy industry and construction. To hold a heavy part without excessive spring deflection, the stiffness of the RCC must be large. If the stiffness of the RCC is large, the insertion forces must also be large, incurring the risk of damaging the parts. Further, commercial RCC devices use elastomer shear pads and have a maximum payload of 400 N in tension, and 53 N in lateral load [14].

In this work we present an alternative approach that fits the environment of those industries where heavy objects are transported with cranes. Instead of holding an object with a compliant structure, we suspend it with multiple cables. Through analysis and experiment, we show that a heavy object can be inserted automatically into a chamfered hole if suspended with multiple cables at particular positions and angles. This is achieved by exploiting the uni-directional load bearing property of cables, where the cables go slack when a compressive load is applied. This property is particularly useful for not over-constraining the peg. The cables can be virtually detached from the peg when they slack, and the multiple cables arranged in a particular configuration can create behaviors similar to that of the RCC hand. However, the principle is different and more importantly from a practical viewpoint, this technology can be used together with cranes and fit the current practice of both heavy industries and the construction industry.

In the following sections, the principle of the cable-suspended peg insertion described, and key conditions for successful insertion will be analyzed with regard to where the multiple cables must be attached. A proof-of-concept prototype is fabricated. And finally, experiments are conducted to demonstrate the effectiveness and verify the analytic conditions on the locations and orientations of multiple-cable attachment.

II. CABLE-SUSPENDED PEG-IN-HOLE INSERTION

The principle of peg insertion using cables is described in this section, followed by static and kinematic analysis. There are three stages involved in peg insertion: the chamfer crossing, one point contact and two point contact, seen in Fig. 2. We aim to obtain conditions for cable arrangements that guide the peg to the hole, while the overhead crane moves the object downward at a constant speed.

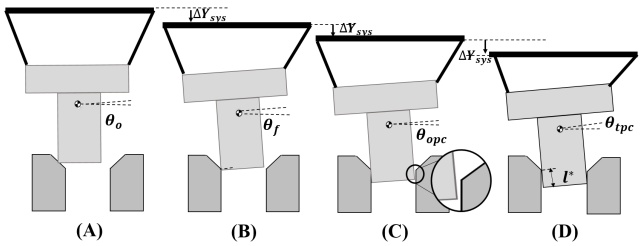

Fig. 2. Stages of peg-in-hole insertion, (A) the first point of contact with the chamfer, (B) the end of the chamfer crossing, (C) one point contact and (D) two point contact. The process of the peg moving from (A) to (B) is called the chamfer crossing. l^* is the depth of the peg within the hole at which two point contact first occurs.

The following assumptions are made:

- The overhead crane moves the heavy object downward at a constant speed without any active control;
- The cable-suspended heavy object moves slowly such that the system can be viewed as quasi-static, governed by static balance of forces and moments;
- The system is symmetric with respect to the vertical centerline of the peg and, thereby, the peg motion is assumed to be constrained within a vertical plane;
- The cables are stiff and inextensible in the longitudinal direction such that the longitudinal elongation is small. The cables can bend flexibly so that they buckle and go slack under compressive loads;
- The hole is placed upright;
- The hole is chamfered; and
- Dimensions of the peg/hole system, including diameters of peg and hole, d, D_h, clearance $D_h - d$, chamfer angle and width, α, W, are known. See Fig. 3.

This work is motivated by a specific application in heavy industry, large gearbox assembly for energy plants, ships and wind turbines. In this application, shaft diameters typically range from 100-300 mm and holes in the gearbox housing have a chamfer width ranging from 3-6 mm. Many modern overhead crane systems used in factory settings [15], [16] can use incremental movements (inching) as small as 2 mm as well as movement speeds as slow as of one percent of the maximum travel speed (microspeed). Therefore, it is reasonable to assume that these systems will be able to place the base frame of the cables within the region of the chamfer of the hole, $\pm W$, as seen in Fig. 1.

Here the goal is to find conditions on cable angles and attachment configuration for successful insertion, given that

the initial misalignment of the peg relative to the hole is within the chamfer width, $\pm W$. In the following analysis we first assume that the hole is perfectly vertical, and analyze the effect of tilt through numerical simulation.

A. No-Slack Insertion

When the peg is crossing the chamfer and entering the hole via one-point-contact, one of the following cases will occur (assuming contact with the left side of the chamfer as depicted in Fig. 2): (1) Right Cable goes Slack, (2) Left Cable goes slack, (3) Neither cable goes slack and (4) Both cables go slack.

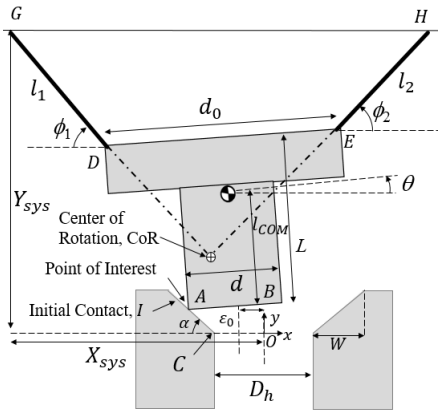

Fig. 3. Geometry definitions for peg-in-hole assembly

Suppose that the right cable goes slack before reaching a two-point contact state when the cable angles are less than 90 degrees, Case (1). The peg receives three forces: the gravity force, one cable tension force, and the contact force from the hole. The contact force may be from a chamfer surface during chamfer crossing, or from the bottom edge of the chamfer during one-point contact. The three forces must balance, if Case (1) is physically possible under the quasi-static process conditions.

The static balance conditions can be examined graphically, as shown in Fig. 4(A) depicting the peg during the chamfer crossing. The lines of action of these three forces must intersect at a single point for a static balance of forces. Considering the friction cone of the contact force, we can find the location of the potential intersection point along the line of action of gravity, indicated with line segment *ab* in the figure. Therefore, the quasi-static balance can be made if the cable applies a tension such that its extension passes through the line segment *ab*. See Fig. 4(A). Instead, if the cable is set with an angle such that it may not intersect with the line segment *ab*, the peg cannot be held quasi-statically with one cable. This implies that the peg can be held only with both cables, that is, Case (3). Therefore, we can assure that both cables do not go slack by directing the cables such that neither cable passes the line segment *ab*.

Under these No-Slack conditions the quasi-static motion of the peg is kinematically determined. As long as both cables are taut, they can be treated as a pair of rigid links. The base frame, the two taut cables, and the peg form a four-bar-linkage within a vertical plane with just one degree of freedom. Fig. 2 shows a peg insertion under the No-Slack conditions. As the peg lands on a chamfer surface, it is constrained by the contact with the chamfer. This means that the peg position and orientation are completely determined by the geometric conditions. As the base frame is lowered, the peg's position and orientation vary in relation to the height of the base frame. After reaching the bottom edge of the chamfer (point C in Fig. 3), the peg contacts the edge of the hole at its side, one-point contact. At this contact state, too, the peg's position and orientation are kinematically determined. This continues until the peg contacts with the hole at two points. Once the peg is constrained by contacts at both sides, the four-bar-linkage is no longer formed. At least one cable must go slack to meet the two-point constraint conditions. The unidirectional nature of cable tension releases the cable, so that the peg may not be over-constrained.

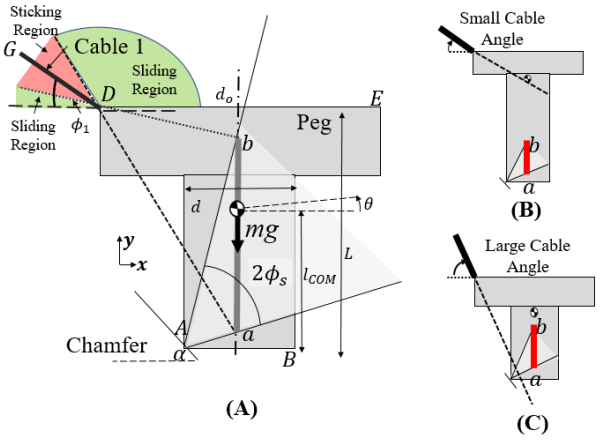

Fig. 4. Region where the tension of the cables and the mass vector of the peg may intersect inside the friction cone during the chamfer crossing. To avoid this region, for long pegs (B), small angles are preferred and for short pegs (C), a large angle cable suspension is desired.

Our strategy for cable-suspended peg insertion is to maintain these No-Slack conditions throughout the insertion process until two-point contact occurs so that the peg movement can be under control kinematically. With proper choice of cable angles and locations of cable attachment, the peg can be guided through the quasi-static process to reach a two-point contact state, which is deep enough to succeed the insertion.

These No-Slack conditions can be met in two regions of cable orientation: one is small angles and the other large angles. In the mid-range, the conditions may be violated. The choice of cable angles depends on the dimensions of a peg. Fig. 4 (B) and (C) illustrates two examples. If the peg is short, a large angle cable suspension is desired, since the lines of cable tension are away from the inhibitory line segment *ab*. On the other hand, if the peg is long, the small angle cable suspension is preferred, since the large angle cable line may interfere with the line segment *ab* as it rotates.

B. Conditions for Successful Insertion

First, consider the necessary conditions for the peg to stick to the chamfer surface. This may occur either at the moment of first contact with the chamfer or while sliding during the chamfer crossing. When it sticks to the surface, the peg loses two degrees of freedom; the only admissible motion is rotation about the point of contact, implying at least one cable must go slack. If the cables are set with a proper angle so that they do not intersect with the line segment *ab* in Fig. 4, there is no chance that the peg can stick to the chamfer surface during the chamfer crossing.

Using the parameters defined in Fig. 4(A), the No-Slack conditions on the angle of cable 1 are given by

$$\tan(\phi_1) \lessgtr \frac{\begin{array}{c} L\cos(\theta)+(\frac{d_o}{2}-\frac{d}{2})\sin(\theta) \\ -(\frac{d}{2}\cos(\theta)-l_{COM}\sin(\theta))\tan(\frac{\pi}{2}-\alpha\mp\phi_s) \end{array}}{(l_{COM}-L)\sin(\theta)-\frac{d_o}{2}\cos(\theta)} \tag{1}$$

A similar, symmetric equation can be derived for cable 2 in the case where cable 1 goes slack. Two sets of cable angle ranges can be calculated for two cases: sticking and sliding. The static coefficient of friction should be used to determine sticking upon first contact with the chamfer and the kinetic coefficient of friction should be used while sliding down the chamfer.

Similar equations can be derived to determine the sticking conditions during one point contact.

It should be noted, however, that no-sticking conditions alone do not guarantee that the peg slides down the chamfer. The peg may stay on the chamfer surface under some kinematic conditions. Fig. 5 shows a case where the peg does not slide, but stays on the chamfer.

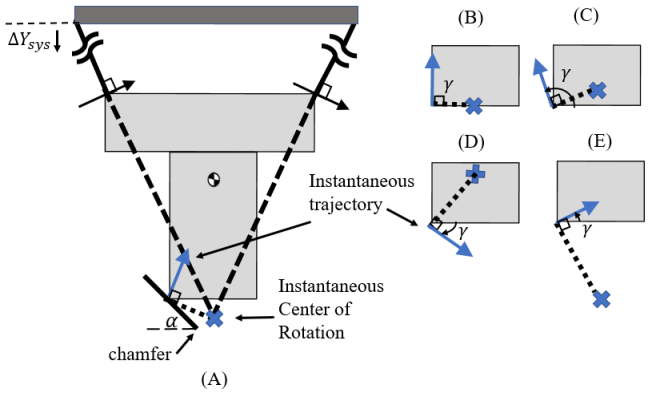

Fig. 5. Center of Rotation determining instantaneous trajectory of the Point of Interest as cable angles change through their range of motion. The small displacement instantaneous trajectory due to the CoR will determine whether the peg will appear stationary (B), move down the chamfer towards the hole (D),(E), or move up the chamfer (C). This relationship between the angle of the instantaneous trajectory and the horizontal axis , γ and the chamfer angle, α, will determine if the peg slides down the chamfer.

At the configuration of (B) in the figure, the instantaneous center of rotation (CoR shown by X) is at the tip of the peg, where the extensions of the two cables intersect. Suppose that the left corner of the peg, point A, touches the chamfer. As the peg rotates about CoR, point A moved upwards. If this upward movement equals the downward movement of the base frame in Fig. 1, the two displacements cancel, and the peg does not slide, but stays stationary on the chamfer. In general, this stationary behavior occurs at a particular relationship among the cable angles, the relative location of point A to the CoR, and the chamfer angle, as shown in Fig. 5.

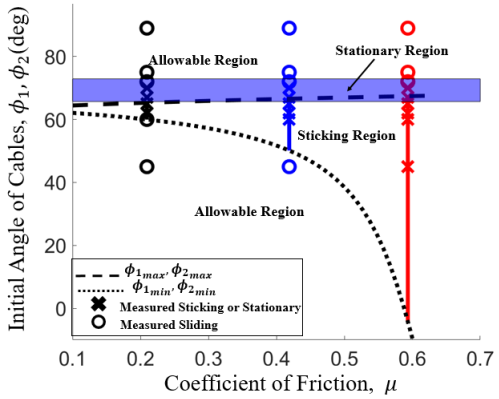

Fig. 6. No-Stick and No-Stationary region for a given peg geometry with experimental verification for three coefficients of friction

Figure 6 represents the sticking and stationary regions graphically. The region between the dashed lines represents the variation of the sticking region as the coefficient of friction, $\mu_s = tan(\phi_s)$ and cable angles, ϕ_1, ϕ_2 are varied. If the selected parameters lie within the sticking region, there is a chance that the peg will stick to the chamfer. The shaded stationary region is determined based purely on the four bar linkage kinematics and is independent of the coefficient of friction. As discussed previously, certain cable angles will result in the peg appearing stationary on the chamfer and can be calculated by examining the peg's instantaneous trajectory. Therefore, for the peg to successfully cross the chamfer, for a known coefficient of friction and setup geometry, the cable angles must be chosen such that result lies within the allowable region of Fig. 6.

At the end of the chamfer crossing, the other side of the peg, point B, must clear the gap. Using four-bar linkage analysis, the final peg tilt angle θ_f can be estimated at the point in which the peg has reached the end of the chamfer and is about to begin the one-point contact state. As eq. (2) describes, if the predicted peg tilt angle meets the specified requirement, the opposite edge of the peg is able to clear the opposite edge of the hole, see Fig. 2.

$$|\theta_f| \ < \tan^{-1}\sqrt{(D_h/d)^2-1} \tag{2}$$

Finally, the peg reaches a two-point contact state when it touches the other side of the hole. The depth of the first two-point contact position, l^* , see Fig. 2, is critically important due to the possibility of the peg to wedge within the hole. Whitney [9] defines wedging as the peg becoming 'stuck'

in the hole due to geometric overlap of the force cones of contact of the peg with the hole and an irreversible failure in the insertion process. If a peg were to wedge in the hole, no correction of applied insertion force is able to force the peg into the hole. Instead, the peg must be entirely removed and the insertion process re-started. Wedging is less likely to occur if the depth at which first two-point contact occurs is sufficiently deep. Depending on the given peg geometry, certain cable mounting angles may yield a deeper depth of first two point contact than others, making wedging less likely. Importantly, then these parameters can be chosen to ensure that the depth of contact is as deep as possible. The depth of first two-point contact is determined from kinematic and geometric conditions, as described next.

III. Peg Trajectory Computation

A. Kinematics Computation

Under the No-Slack conditions, the peg trajectory can be computed from kinematic conditions. Since both cables are taut the following equations must be true,

$$\begin{aligned}(x_G - x_D)^2 - (y_G - y_D)^2 &= l_1^2 \\ (x_H - x_E)^2 - (y_H - y_E)^2 &= l_2^2\end{aligned} \tag{3}$$

where $(x_G, y_G), (x_D, y_D), (x_E, y_E)$ and (x_H, y_H) are coordinates of points G, D, E, and H, respectively. See Fig. 3.

When the peg is on a chamfer surface, it must satisfy another constraint given by

$$(x_A + \frac{D_h}{2})\sin\alpha + y_A \cos\alpha = 0 \tag{4}$$

At a one-point contact state with positive peg tilt and cable angles less than 90 degrees, it must satisfy:

$$y_C - (y_D + \frac{d_0 - d}{2})\sin\theta = -x_C + (x_D + \frac{d_0 - d}{2})\sin\theta \tag{5}$$

where the coordinates of C are $(x_C, y_C) = (-D_h/2, 0)$, as well as the inequality

$$x_B \leq D_h/2 \tag{6}$$

so that point B on the peg does not intersect the right wall of the chamfer.

In each case, there are three unknowns, the peg position and orientation, and three constraint equations with one inequality constraint (6). We apply the well known Freudenstein equations for four bar linkages [17] to compute the peg configurations at key stages during the insertion process.

B. Simulation

The No-Slack insertion method entails that both cables are kept taut throughout the process. This can be examined through simulation. First, the system is displaced downward by a small amount. Then the new position of the peg is determined based upon the four-bar linkage kinematics. Then, the free body diagram analysis is conducted for the system to remain in static equilibrium. If either cable is determined to be in compression in order for the desired configuration to be achieved or if the normal force acting from the chamfer is negative, the configuration is determined to be infeasible for a four-bar linkage and the given cable mounting angles yield an infeasible solution. This process can be repeated for all desired mounting angles that are within the allowable range from Fig. 6. This computational procedure can be extended to determine l^*, the depth at which first two-point contact can occur.

C. Parameter Study

The predicted peg trajectories depend on several parameters of the system. Particularly important is to examine how varying the length of the peg, L, the diameter of the peg, d, and the chamfer angle, α, effects the predicted sticking and stationary regions and how the tilt of the hole, γ, effects the predicted peg angle at the end of the chamfer crossing and depth of first two point contact. The results can be seen in Fig. 7.

As peg length L is increased, Fig. 7(A), the region of initial cable angles in which the sticking phenomena may occur shifts towards higher cable angles, and the region in which the peg will appear stationary, too, shifts higher. This implies that small cable angles are desired, as shown in Fig. 4-(B). As the peg width d increases, Fig. 7(B), the sticking phenomena may occur in a broader range of cable angles, while the stationary region remains roughly the same. As the chamfer angle becomes less steep, Fig. 7(C), the peg becomes more likely to stick to the chamfer and appear stationary as well.

In a practical factory setting, it is difficult to place a hole in a perfectly vertical direction. Let γ be the angular misalignment of the hole. We can predict the depth of first two point contact, l^*, by tilting the walls of the hole in the previous simulation model. Fig. 8 shows an example of the predicted l^* for the short peg, $L = l^*$. As the misalignment angle increases, l^* decreases in general. Note that those of large cable angles, although producing deeper l^* for small misalignment, tend to be more susceptible to the angular misalignment. It should be noted that this parameter study was conducted with multiple values of peg/hole clearance $(150, 200, 370)$, and the trends were the same as the one shown.

IV. Experimental Verification

The proposed insertion method and the analytical results were validated through experiments using both 2D and 3D scale models. As seen in Fig. 9, two steel pegs were manufactured to slide into a steel hole with a chamfer angle of 45 degrees. The bottom corners of the pegs were given a fillet of 0.6 mm. The pegs were connected to the mounting system via low-stretch polyester rope of length 215.9 mm and the mounting system was attached to a linear guide rail that was powered by a lead screw. Indicator LEDs provide a trigger as to when the first two-point contact occurred. Various types of material were placed on the chamfer surface to vary the coefficient of friction of the interaction between the peg and the chamfer.

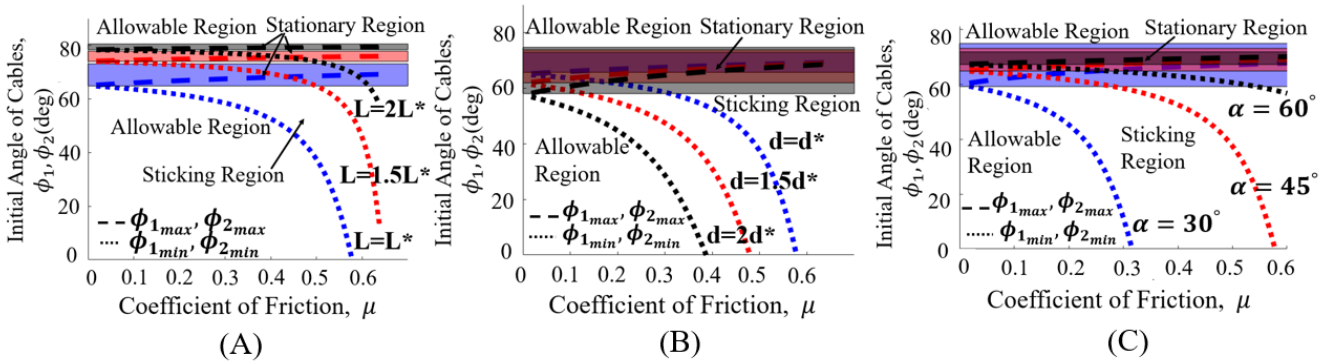

Fig. 7. Parameter sweep for determining change of allowable cable placement angles for given peg geometry, peg-chamfer coefficient of friction as (A) the peg length, L is increased, (B) the peg width, d is increased, (C) the chamfer angle α is varied. d^*, L^* and $\alpha = 45$ deg are the nominal parameters used in the physical experimental setup described in section IV.

For the purpose of experimental validation of the analytical results, OptiTrack motion capture systems [18], [19] and AprilTags [20], were used for tracking the position and orientation of the peg. This motion tracking is only for laboratory use, and is not required for actual implementation of this strategy. The preliminary experiment of position measurement accuracy revealed that the OptiTrack and AprilTag systems possessed a mean positioning error of 0.183 mm and 0.68 mm and rotational error of 0.09 and 0.28 degrees, respectively.

First, an experiment was conducted to verify the successful chamfer crossing of the peg when the cable angles are in both allowable and not-allowable regions dictated by the no-stick and no-stationary conditions using three different coefficients of friction. See Fig. 6. This experiment was conducted using a 101.6 mm length peg with a hole clearance of 1 mm. As the coefficient of friction of the peg-hole system increases, the range for allowable initial values of ϕ_1, ϕ_2, decreases drastically. This experiment showed that the peg was seen to be sliding only in the allowable region and that it was either stuck due to friction or due to four bar linkage kinematics in the not-allowable region. In the previous analysis, two

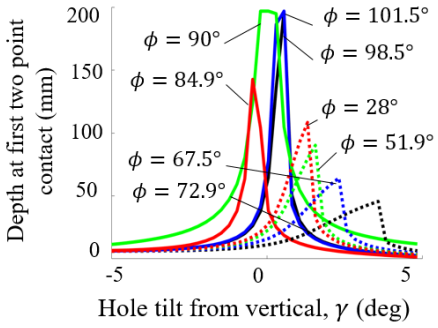

Fig. 8. Parameter sweep for determining depth of first two point contact as the hole is tilted by angle γ from vertical. d^*, L^* and $\alpha = 45$ deg are the nominal parameters used in the physical experimental setup described in section IV.

critical quantities were obtained. One is the depth of insertion at first two-point contact l^*, and the other is the peg tilt angle at the end of chamfer crossing θ_f. Fig. 10 presents experimental measurements of l^* and θ_f, compared to the analytic results shown by solid curves. Three experimental setups were used; a 101.6 mm long peg with a hole clearance of 1.0 mm, a 101.6 mm long peg with a hole clearance of 0.2 mm, and a 203.2 mm long peg and a hole clearance of 0.37 mm. Experiments were conducted for different horizontal misalignment of the peg and different cable angles. For all three setups, horizontal errors, ε_0, of 1.27 mm in red, 2.54 mm in blue and 5.08 mm in black, which represent 2.5%, 5% and 10% of the diameter of the peg respectively, were used. Each small circle in the figure represents the average value of five trials under the same conditions. Error bars show the range of variability of measurements. For most of the data the variability is so small that the error bars are within the small circles.

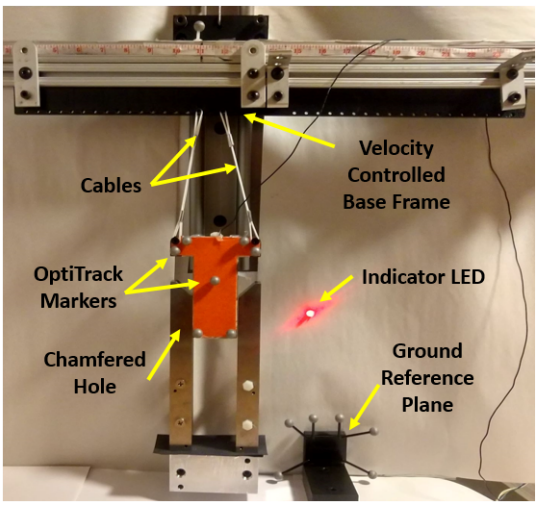

Fig. 9. Experimental Setup for 2D Cable Suspended Peg Insertion Experiments

In general, as the cable angles become closer to the prohibitory sticking/stationary region shown in black, the depth l^* decreases and the tilt angle θ_f increases, making insertion

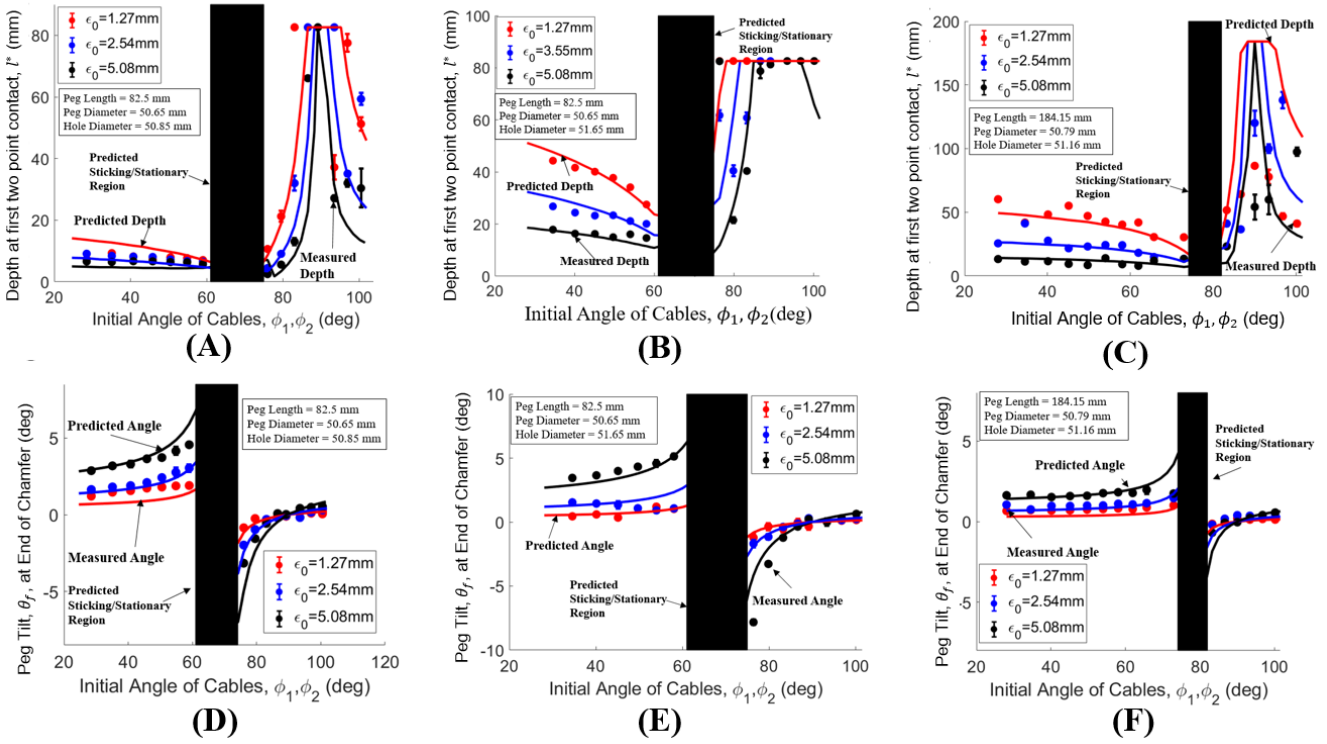

Fig. 10. Predicted and Measured depth of first two point contact (A-C) and predicted and peg tilt at the end of the chamfer crossing (D-F) for three experimental cases. The first experimental setup, (A)(D), uses a peg length of 101.6 mm and a clearance of 0.2 mm. The second experimental setup, (B)(E), uses a peg length of 101.6 mm and a clearance of 1 mm. The third experimental setup (C)(F) uses a peg length of 203.2 mm and a clearance of 0.37 mm.

TABLE I
SUMMARY OF EXPERIMENTAL RESULTS FOR FOUR-BAR LINKAGE MODEL VERIFICATION

			RMSE					
			$\varepsilon_0 = 1.27mm$		$\varepsilon_0 = 2.54mm$		$\varepsilon_0 = 5.08mm$	
Exp. No.	Peg length (mm)	$D_h - d$ (mm)	θ_f (deg)	l^* (mm)	θ_f (deg)	l^* (mm)	θ_f (deg)	l^* (mm)
1	101.6	.2	0.8	16.7	1.3	14.3	2.4	12.7
2	101.6	1	0.6	2.5	1.2	11.9	3.6	19.9
3	203.2	.37	0.5	66.2	0.8	44.1	1.4	56.5

difficult. At the cable angles of 90 degrees, l^* increases and θ_f decreases. However, the error bands of the depth becomes longer, indicating higher variability. This agrees with the results of Fig. 8; the depth l^* varies significantly depending on the hole tilt angle γ, indicating that the cable angle of 90 degrees is susceptible to the angular misalignment of the hole. In contrast, smaller cable angles are more consistent and less sensitive to the hole angular misalignment. This is particularly significant for the longer peg, 203.2 mm. Small cable angles yield more uniform l^*.

Table I summarizes the prediction accuracy of the analytic model compared to the experimental results. Overall, the model can predict the experimental results satisfactorily.

Further, additional trials were conducted using a 3D setup (see Fig. 11) consisting of a 3.5 kg aluminum round peg that is 101.7 mm in diameter and 152.4 mm long, an aluminum hole with an inner diameter of 101.85 mm, low-stretch polyester ropes that are 457 mm and 609.6 mm long, and a mounting plate that is 203.2 mm in diameter. The clearance is 0.15 mm. In Fig. 11, the origin corresponds to the position where the peg is fully inserted in the hole. The distance between the center of the peg and the center of the hole indicates the magnitude of the horizontal distance between the radial axis of the peg and the hole.

The results of the trials, depicted in Fig. 11, show that for certain cable angles, the peg does not successfully cross the chamfer and enter the hole.

In these cases, the peg tips 'forward' and essentially topples over and the graph is depicted by a significant change in the distance of the center of the peg to the center of the hole and no progress of insertion. The peg insertion is successful when the cables are outside this range, specifically when they are mounted at 76 deg and 38 deg from horizontal. This is depicted in Fig. 11 by the lines that simultaneously make progress towards being fully inserted in the hole and the centers of the hole and peg come into alignment. This further verifies the results depicted in the 2D simulations and experiments.

V. CONCLUSION AND FUTURE WORK

The aforementioned work proposed to develop a novel technique for the assembly of heavy objects, specifically the peg-in-hole problem, using a multi-cable suspended robotic system. Key conditions were derived for a peg to be passively

inserted into a hole using fixed length cables and exploiting the ability of cables to go slack to avoid over-constraint.

Both analytical and experimental results have shown that there are two primary ranges in which passive cable-suspended peg insertion may be possible. The first region, where the cables are nearly vertical and the second where the cable mounting angles are small, $> 85deg$ and $< 55deg$ for our specific experimental conditions. However, with each region comes conflicting challenges. When the cables are nearly vertical, the peg can reach the end of the chamfer with a small peg tilt and the depth of first two-point contact is predicted to be large. However, it is more susceptible to the angular misalignment of the hole. Furthermore, the peg is much more susceptible to sway with a large magnitude due to perturbations during transportation by a crane. When the cable angles are small, the peg tilt will be larger as it reaches the end of the chamfer and the depth of two-point contact is predicted to be smaller. However, the system is less susceptible to the angular misalignment of the hole as well as to disturbances during the crane transportation. These present a design trade off that the user must examine based upon specific conditions of the application. The objective

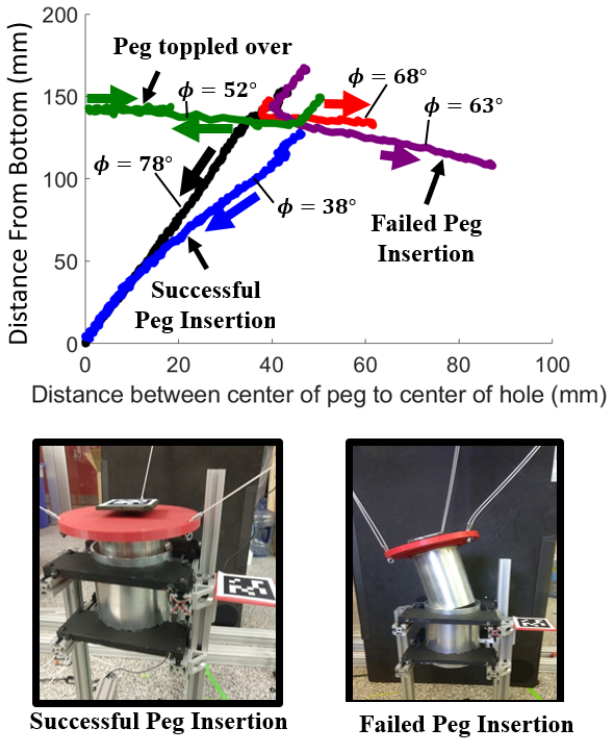

Fig. 11. Experimental trials using the 3D setup. The trials with cables in the range of 52-68 deg resulted in the peg failing the chamfer crossing. The trials with a large cable angle, 78 deg, and a small cable angle, 38 deg, were successfully able to cross the chamfer and fully insert into the hole.

of the insertion analysis, including the parameter study, and the experimental verification is to provide guidelines for successful insertion. Given dimensions of a peg and a hole we have obtained how to best choose parameters that have been shown to lead to a predictable depth of first two-point contact which can be used to predict successful insertion. Although the method proposed in this paper is mainly valid for environments in which misalignment and uncertainty are quantifiable, it can be improved upon by incorporating feedback control mechanisms, such as winches to control cable length or linear actuators to control cable angle positioning, to compensate for disturbances and modeling errors. This type of control is intended to be explored in future works.

REFERENCES

[1] Elka Torpey, "Got skills? Think manufacturing : Career Outlook: U.S. Bureau of Labor Statistics," 2014. [Online]. Available: https://www.bls.gov/careeroutlook/2014/article/manufacturing.htm

[2] "Kr 600 fortect," http://https://www.kuka.com/en-us/products/robotics-systems/industrial-robots/kr-600-fortec, accessed: 2019-12-09.

[3] Z. B. S. W. X. Q. Qian, S., "A Review on Cable-driven Parallel Robots," *Chinese Journal of Mechanical Engineering*, vol. 31, no. 66, Aug 2018.

[4] J. S. Albus, R. V. Bostelman, and N. G. Dagalakis, "The NIST ROBOCRANE — NIST," *Journal of Robotics System*, vol. 10, No. 5, sep 1992. [Online]. Available: https://www.nist.gov/publications/nist-robocrane

[5] M. Gouttefarde, J.-F. Collard, N. Riehl, and C. Baradat, "Geometry Selection of a Redundantly Actuated Cable-Suspended Parallel Robot," *IEEE Transactions on Robotics*, vol. 31, no. 2, pp. 501–510, apr 2015. [Online]. Available: http://ieeexplore.ieee.org/document/7050380/

[6] N. G. Dagalakis, J. S. Albus, B. Wang, J. Unger, and J. W. Lee, "Stiffness Study of a Parallel Link Robot Crane for Shipbuilding Applications," feb 1988. [Online]. Available: https://www.nist.gov/publications/stiffness-study-parallel-link-robot-crane-shipbuilding-applications

[7] T. Higuchi, A. Ming, and J. Jiang-Yu, "Application of Multi-Dimensional Wire Cranes in Construction," jun 1988.

[8] K. Saidi, A. Lytle, W. Stone, and N. Scott, "Developments toward an autonomous robotic crane for automated steel construction," *NISTIR*, no. 7264, 2003.

[9] D. E. Whitney, "Quasi-Static Assembly of Compliantly Supported Rigid Parts," *Journal of Dynamic Systems, Measurement, and Control*, vol. 104, no. 1, pp. 65–77, mar 1982.

[10] S. N. Simunovic, "An information approach to parts mating," *Sc.D. Thesis,Mechanical Engineering Department, and published as CSDL Report T-690, April 1979.*, 1979.

[11] J. Nevins and D. Whitney, "Assembly research," *Automatica*, vol. 16, no. 6, pp. 595–613, nov 1980. [Online]. Available: https://www.sciencedirect.com/science/article/pii/0005109880900035

[12] S. Drake and S. N. Simunovic, "Compliant Assembly Device," *United States Patent 4, 144, 169*, 22, May 1979.

[13] J. Xu, Z. Hou, Z. Liu, and H. Qiao, "Compare contact model-based control and contact model-free learning: A survey of robotic peg-in-hole assembly strategies," 2019.

[14] A. I. Automation, "Compliance Device Models," accessed 2020-02-12. [Online]. Available: https://www.ati-ia.com/products/compliance/Compensator_Models.aspx

[15] Konecrane, "Intelligent lifting with Safe Features," accessed 2020-05-27. [Online]. Available: https://www.konecranes.com/resources/smart-features

[16] SWF Krantechnik, "Crane Components CraneKits: NOVA Blackline," accessed 2020-05-27. [Online]. Available: https://www.swfkrantechnik.com/en/products/crane-kit-blackline/

[17] F. Freudenstein, "Design of four-link mechanisms," Ph.D. dissertation, Columbia University, New York City, NY, 1954.

[18] OptiTrack, "Flex 3," accessed 2020-05-27. [Online]. Available: https://optitrack.com/products/flex-3/

[19] NaturalPoint Inc., "Motive: Optical motion capture software," accessed 2020-05-27. [Online]. Available: https://optitrack.com/products/motive/

[20] E. Olson, "Apriltag: A robust and flexible visual fiducial system," in *2011 IEEE International Conference on Robotics and Automation*, 2011, pp. 3400–3407.